JACS
JOURNAL OF THE AMERICAN CHEMICAL SOCIETY
pubs.acs.org/JACS
Communication

Site-Selective Surface Modification of 2D Superatomic Re_6Se_8

Shoushou He, Austin M. Evans, Elena Meirzadeh, Sae Young Han, Jake C. Russell, Ren A. Wiscons, Amymarie K. Bartholomew, Douglas A. Reed, Amirali Zangiabadi, Michael L. Steigerwald,* Colin Nuckolls,* and Xavier Roy*

Cite This: *J. Am. Chem. Soc.* 2022, 144, 74−79
Read Online
ACCESS | Metrics & More | Article Recommendations | Supporting Information

ABSTRACT: Coating two-dimensional (2D) materials with molecules bearing tunable properties imparts their surfaces with functionalities for applications in sensing, nanoelectronics, nanofabrication, and electrochemistry. Here, we report a method for the site-selective surface functionalization of 2D superatomic $Re_6Se_8Cl_2$ monolayers. First, we activate bulk layered $Re_6Se_8Cl_2$ by intercalating lithium and then exfoliate the intercalation compound $Li_2Re_6Se_8Cl_2$ in *N*-methylformamide (NMF). Heating the resulting solution eliminates LiCl to produce monolayer $Re_6Se_8(NMF)_{2-x}$ ($x \approx 0.4$) as high-quality nanosheets. The unpaired electrons on each cluster in $Re_6Se_8(NMF)_{2-x}$ enable covalent surface functionalization through radical-based chemistry. We demonstrate this to produce four previously unknown surface-functionalized 2D superatomic materials: $Re_6Se_8I_2$, $Re_6Se_8(SPh)_2$, $Re_6Se_8(SPhNH_2)_2$, and $Re_6Se_8(SC_{16}H_{33})_2$. Transmission electron microscopy, chemical analysis, and vibrational spectroscopy reveal that the in-plane structure of the 2D Re_6Se_8 material is preserved through surface functionalization. We find that the incoming groups control the density of vacancy defects and the solubility of the 2D material. This approach will find utility in installing a broad array of chemical functionalities on the surface of 2D superatomic materials as a means to systematically tune their physical properties, chemical reactivity, and solution processability.

Technologies based on two-dimensional (2D) materials rely on the predictable manipulation of their physical and chemical properties. A promising approach to create diverse and useful 2D materials is to chemically modify their exposed surfaces.[1−4] While the characteristics (*e.g.*, solubility, optical emission, photovoltaic effect) of conventional 2D materials such as transition-metal dichalcogenides (TMDCs) have been modulated through surface modification,[5−7] these interfacial reactions nearly always produce low grafting densities, high defect densities, and poor site-selectivities—all of which degrade the electrical, mechanical, and optical properties of the materials.[8,9] The recent emergence of layered structures assembled from tailorable superatomic clusters has significantly expanded the structural complexity of 2D materials, opening the door to new chemistry for surface functionalization.[10−13] Exciting properties such as superconductivity arise as the surface structure of 2D superatomic materials is tuned.[14]

In this work, we detail a method for the surface functionalization of such 2D superatomic materials that is chemically general and achieves a high degree of surface coverage. Even though there are many examples of isolated clusters that feature ligand exchange in solution,[15−17] our work unprecedentedly showcases surface functionalization of a 2D superatomic material. Our strategy centers around our ability to quantitatively exchange the surface-capping chlorine atoms from $Re_6Se_8Cl_2$ nanosheets. The effective homolytic cleavage of I_2 and RS−SR produces iodine (I) and sulfur-based (SR) radicals that react with the 2D Re_6Se_8 surfaces (Figure 1). Vibrational spectroscopy and energy-dispersive X-ray spectroscopy (EDX) confirm that the radical-based functionality can completely replace the surface-capping chlorine from $Re_6Se_8Cl_2$ nanosheets. High-resolution scanning transmission electron microscopy (HR-STEM) reveals that the resulting 2D $Re_6Se_8I_2$, $Re_6Se_8(SPh)_2$, $Re_6Se_8(SPhNH_2)_2$, and $Re_6Se_8(SC_{16}H_{33})_2$ all retain the in-plane crystal structure of the parent compound. However, we find that the density of superatom cluster vacancy defects depends strongly on the incoming functional groups. We have developed an automated postprocessing approach to quantify defect vacancy across many HR-STEM images, which enables us to conclude that the $Re_6Se_8(SC_{16}H_{33})_2$ has the lowest defect density of 1 cluster vacancy in 2000 (0.05%). This chemically general approach enables the high-fidelity surface modification of 2D superatomic materials.

Unlike TMDCs, which are atomic lattices, $Re_6Se_8Cl_2$ is comprised of Re_6Se_8 superatomic building blocks.[10] In a Re_6Se_8 cluster, the Se atoms reside on the faces of the Re_6 octahedron. The Re_6Se_8 clusters are covalently bonded along the *a* and *b* crystallographic directions to form a 2D pseudosquare lattice. The *trans*-Re atoms in the 2D sheets are capped by Cl atoms at the apical positions. The 2D $Re_6Se_8Cl_2$ layers stack on top of one another to form a bulk van der Waals structure that can be intercalated and exfoliated (Figure 1). We prepare bulk microcrystalline $Re_6Se_8Cl_2$ by

Received: October 13, 2021
Published: January 3, 2022

https://doi.org/10.1021/jacs.1c10833
J. Am. Chem. Soc. 2022, 144, 74−79

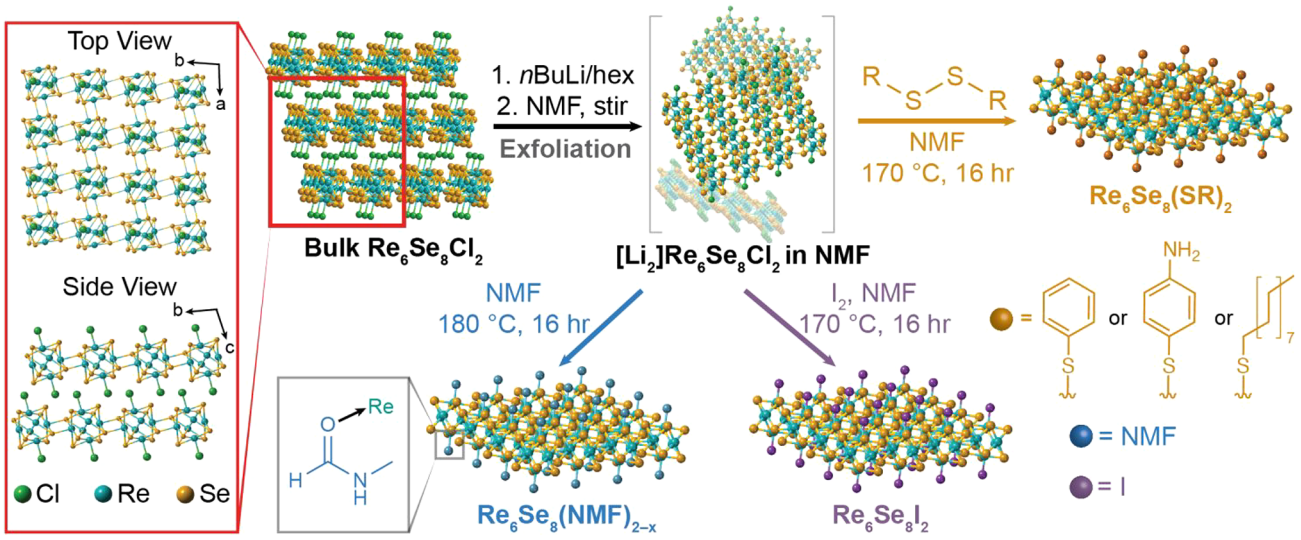

Figure 1. Crystal structure of $Re_6Se_8Cl_2$ and its activation by Li intercalation followed by subsequent surface modification through the homolytic cleavage of functionalizing reagents. The atomic positions of Li in the exfoliated $Li_2Re_6Se_8Cl_2$ sheets are not specified.

heating a stoichiometric mixture of Re, Se, and $ReCl_5$ at 1100 °C in a fused silica tube sealed under vacuum for 72 h (see the Supporting Information for the complete procedure).[18,19] As has previously been reported, Li can be intercalated into the interlayer spacing of $Re_6Se_8Cl_2$ electrochemically.[20] In our synthesis, we Li-intercalate $Re_6Se_8Cl_2$ by treating $Re_6Se_8Cl_2$ in a 0.16 M solution of *n*-butyllithium, yielding $Li_2Re_6Se_8Cl_2$, as confirmed by inductively coupled plasma−optical emission spectroscopy (ICP-OES) (Table S1).[18] Following lithium intercalation, $Li_2Re_6Se_8Cl_2$ exfoliates in *N*-methylformamide (NMF) to form a stable colloid. These exfoliated $Li_2Re_6Se_8Cl_2$ nanosheets serve as the starting material for surface modification.

We initiate surface functionalization by heating $Li_2Re_6Se_8Cl_2$ at 180 °C in NMF for 16 h to completely remove the Cl from the surface of nanosheets (presumably as LiCl), cap the nanosheets with NMF, and isolate $Re_6Se_8(NMF)_{2-x}$; the TGA results indicate that x is ∼0.4 (Figure S1). Li and Cl are absent in ICP-OES and EDX of $Re_6Se_8(NMF)_{2-x}$ (Figure S2).[21] On the basis of the EDX data, we determine that the Re and Se compositions in the 2D Re_6Se_8 framework remain unchanged after Cl removal (Figure 2A). NMF is unique for this process; we attempted this transformation in many other solvents (including *N*,*N*-dimethylformamide, dimethyl sulfoxide, amines, ethers, and H_2O) and none allowed for an efficient liquid exfoliation and Cl removal. We suspect that this is due to the very high dielectric constant of NMF (182.4 at 25 °C).[22]

Fourier-transform infrared spectroscopy (FT-IR) reveals that the NMF datively coordinates to the Re atoms on the 2D Re_6Se_8 surface in $Re_6Se_8(NMF)_{2-x}$ (Figure 2B). In comparison to the unbound NMF, the C═O stretching band shifts to a lower frequency in $Re_6Se_8(NMF)_{2-x}$ (1673 to 1644 cm^{-1}), whereas the amide C−N antisymmetric stretching band shifts to a higher frequency (1548 to 1562 cm^{-1}). The decrease in C−O bond order and increase in C−N bond order indicate a contribution from the zwitterionic amide resonance form, which facilitates the donor−acceptor interactions between the carbonyl oxygen of NMF and Re.[23] The results are consistent with the previous reports of O-coordinated NMF.[24] Thus, the experimental vibrational shifts indicate that NMF is bound to the Re atoms by dative interactions through its carbonyl oxygen, and we see no evidence of unbound NMF. As we will discuss below, the in-plane structure of $Re_6Se_8(NMF)_{2-x}$ remains intact.

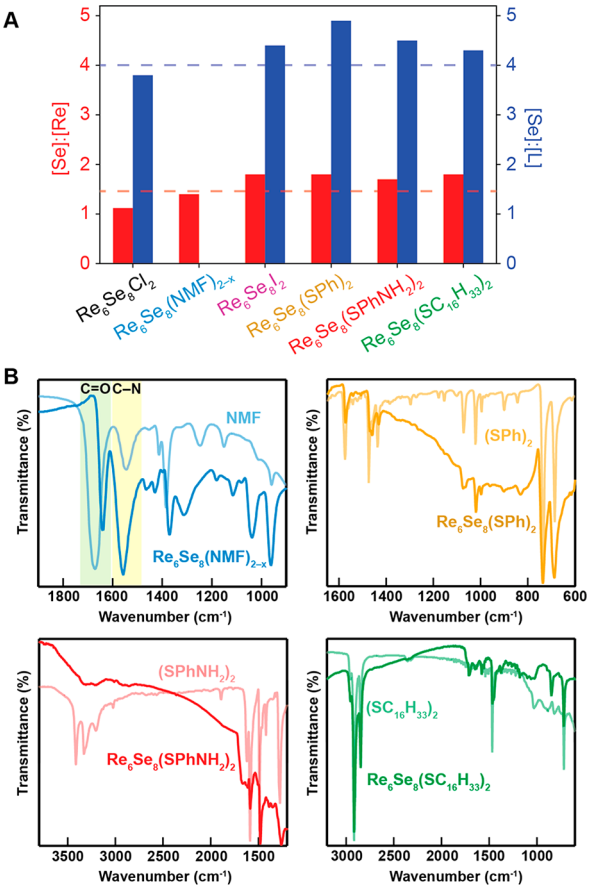

Figure 2. (A) Experimental [Se]:[Re] and [Se]:[L] ratios based on the atomic percentages obtained from EDX, where L is Cl, I, or S. The red and blue dashed lines indicate the expected [Se]:[Re] and [Se]:[L] ratios of $Re_6Se_8L_2$, respectively. (B) FT-IR spectra of the surface-functionalized 2D Re_6Se_8 materials (darker) and surface-modifying reagents (lighter). We focus on diagnostic regions of the spectra for each surface functionality.

https://doi.org/10.1021/jacs.1c10833
J. Am. Chem. Soc. 2022, 144, 74−79

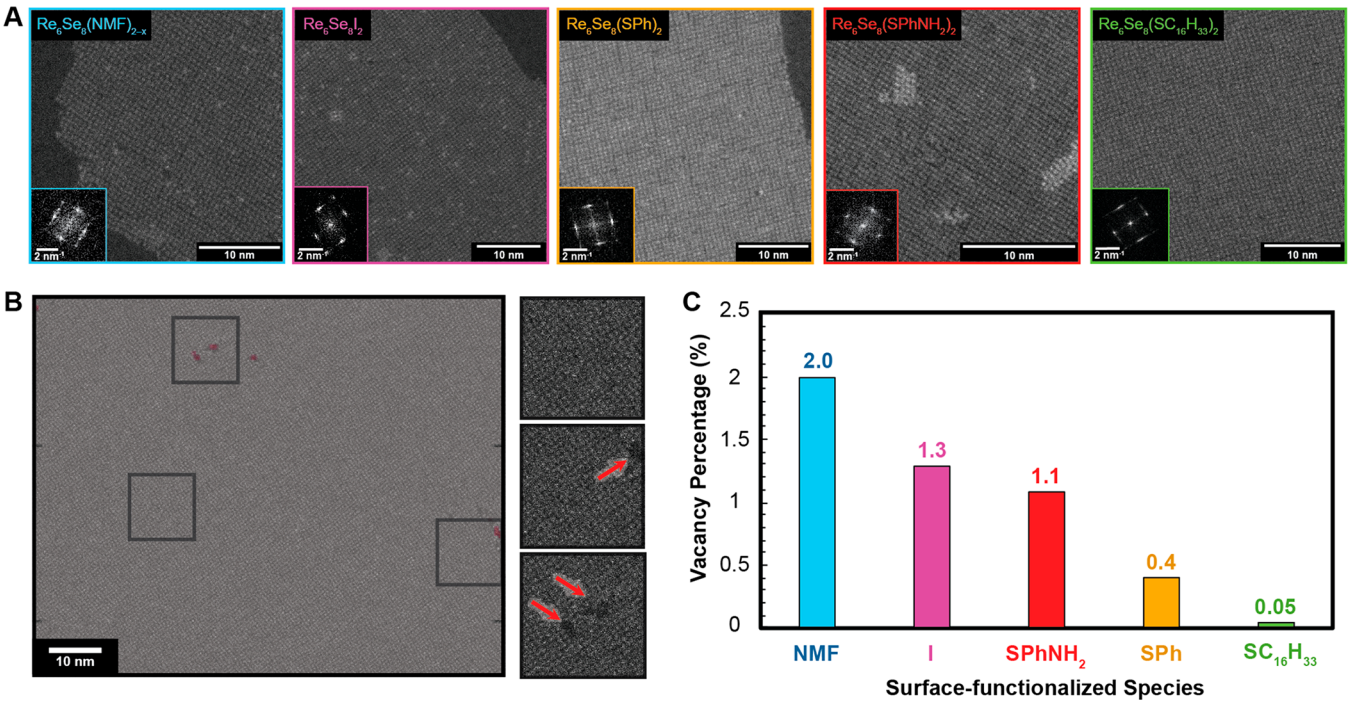

Figure 3. (A) HR-STEM images of the new surface-functionalized 2D Re_6Se_8 materials. The insets show the fast Fourier transform (FFT) of the HR-STEM images. (B) Defect analysis of an HR-STEM image of a $Re_6Se_8(SC_{16}H_{33})_2$ monolayer. (C) Bar graph summarizing the cluster vacancy percentages of the surface-functionalized 2D Re_6Se_8 materials.

When they are taken together, the elemental analysis and FT-IR results suggest that each intercalated lithium in $Li_2Re_6Se_8Cl_2$ transfers one electron to the 2D Re_6Se_8 layers, yielding each $Li_2Re_6Se_8Cl_2$ subunit as $[Re_6Se_8Cl_2]^{2-}$ paired with two Li^+ counterions. As was previously described, the equivalents of Li^+ and an electron are introduced into solid-state lamellar materials after treatment with *n*-butyllithium, while the butyl radicals react to form hydrocarbon by-products.[25,26] LiCl removal leaves each Re_6Se_8 cluster subunit reduced by two electrons in comparison to the all-Re^{III} starting material; the resulting cluster can be thought of as functionally consisting of four Re^{III} and two Re^{II} atoms. This led us to hypothesize that the unpaired electrons on Re^{II} centers would participate in one-electron chemistry with homolytically cleavable reagents. Indeed, our experimental results indicate that the 2D Re_6Se_8 surfaces react with one-electron species.

We can use many reactants to functionalize the surface of Re_6Se_8 nanosheets. To replace the surface-capping Cl atoms, we heat $Li_2Re_6Se_8Cl_2$ in the presence of a homolytically cleavable molecule in NMF at 170 °C for 16 h. For instance, by heating $Li_2Re_6Se_8Cl_2$ in the presence of I_2 the Cl atoms are replaced with I, thus yielding $Re_6Se_8I_2$, a previously unreported 2D superatomic material. A 3D $Re_6Se_8I_2$ polymorph has been recently synthesized as the thermodynamic product in the solid state.[27] Our solution-based surface functionalization allows us to obtain the 2D $Re_6Se_8I_2$ monolayers that are inaccessible by traditional high-temperature routes. In none of the EDX spectra of surface-modified Re_6Se_8 do we observe any Cl signal, indicating its complete removal (Figure S3). Moreover, the EDX spectrum of $Re_6Se_8I_2$ reveals that the Cl to I exchange is quantitative while the Re_6Se_8 composition is left unchanged, as indicated by the close correlation between the experimental and expected [Se]:[I] and [Se]:[Re] ratios for $Re_6Se_8I_2$ (Figure 2A and Table S2).[28] As we will discuss below, the in-plane structure of $Re_6Se_8I_2$ is intact after site-selective surface modification. These results with I_2 inspired our investigation into the reactivity of $Li_2Re_6Se_8Cl_2$ with disulfides (diphenyl disulfide, 4-aminophenyl disulfide, and dihexadecyl disulfide) that we expected would cleave homolytically.

EDX and FT-IR spectroscopy verify complete site-selective substitution of Cl for SR (R = Ph, 4-NH_2Ph, $C_{16}H_{33}$) (Figures S4−S6). We also measured the atomic compositions of Re, Se, and S using EDX (Table S2) and calculated the [Se]:[Re] and [Se]:[S] atomic percentage ratios (Figure 2A). The experimental [Se]:[Re] ratios of $Re_6Se_8(SR)_2$ correlate well with the expected ratio corresponding to Re_6Se_8 ([Se]:[Re] = 4:3), thus indicating that the compositions of the 2D framework remain unchanged after surface modification. We find that the Cl to SR exchange is nearly stoichiometric as well because the experimental [Se]:[S] ratios all fall within acceptable error of the expected value ([Se]:[L] = 4:1; Figure 2A).[29] In all cases, FT-IR spectra of $Re_6Se_8(SR)_2$ structures show that the −SR moiety remains intact (Figure 2B and Figure S7), suggesting that Re−SR bonding is likely responsible for surface functionalization. This is further supported by the fact that diphenyl sulfide, which cannot homolytically cleave, does not bind to the surface of Re_6Se_8. Thus, we conclude that surface functionalization proceeds via a radical process that leads to covalent Re−SR bond formation. We note that the NH_2 vibrational bands at 3500−3000 cm^{-1} for $Re_6Se_8(SPhNH_2)_2$ are broader and less resolved in comparison to the bands of $NH_2PhS-SPhNH_2$; this is most likely due to the different hydrogen-bonding environments in $Re_6Se_8(SPhNH_2)_2$ and $NH_2PhS-SPhNH_2$.

The functionalized nanosheets suspended in NMF can be recovered as a dark gray powder by precipitation (see the Supporting Information for details). Powder X-ray diffraction (PXRD) of the solids shows that the interlayer spacings for the

https://doi.org/10.1021/jacs.1c10833
J. Am. Chem. Soc. 2022, 144, 74−79

surface-functionalized materials are greater than the interlayer spacing of bulk $Re_6Se_8Cl_2$ (Figure S8 and Table S3), consistent with the addition of steric bulk on the functionalized 2D Re_6Se_8 surface. Since the (001) diffraction peaks are broad for all of the functionalized materials (Figure S8), we conclude that the long-range stacking order is compromised after surface functionalization. Nonetheless, PXRD provides initial evidence that the 2D Re_6Se_8 structure is intact after surface modification because the broad feature centered at $2\theta = 14.3°$ is present in the patterns of all functionalized materials; this feature is diagnostic of the in-plane periodicity, as it comes from overlapping (010) and (100) peaks in the PXRD pattern of pristine $Re_6Se_8Cl_2$. These results prompted us to image the in-plane structure of the surface-functionalized materials using HR-STEM.

HR-STEM reveals that the stoichiometric substitution of chlorine for NMF, iodine, and the sulfur-based radicals preserves the 2D structure formed by covalently linked Re_6Se_8 clusters (Figure 3A). The well-defined fast Fourier transform (FFT) patterns of the nanosheets verify that the in-plane crystallinity is preserved after surface functionalization (Figure 3A, insets). Also, the lattice dimensions derived from the FFTs (6.4 Å) align with those of the $Re_6Se_8Cl_2$ crystal structure (6.6 Å), indicating the cluster arrangements remain largely unchanged after surface functionalization. We performed an automated high-throughput postprocessing analysis of STEM images to characterize the density of superatom vacancies (Figure 3B). Using this method, we analyzed 25 images, corresponding to a micrometer scale and statistically relevant mapping areas. By an autonomous examination of image contrast differences, the screening program can identify the locations of Re_6Se_8 cluster vacancies. After site-selective surface modification, the 2D nanosheets all exhibit robust structural integrity with cluster vacancy percentages ranging from 2.0% to 0.05% for $Re_6Se_8(NMF)_{2-x}$ and $Re_6Se_8(SC_{16}H_{33})_2$, respectively (Figure 3C). While all of the surface-functionalized materials shown here are nearly pristine, we find it fascinating that the defect levels vary with different surface functionalities.

Surface functionalization drastically modifies the colloidal stability of 2D Re_6Se_8 nanosheets, as highlighted by Tyndall scattering in Figure 4. In these images, scattering of the red laser indicates the presence of suspended nanosheets in the solvent. $Li_2Re_6Se_8Cl_2$ only exfoliates and dissolves in NMF, which limits the subsequent chemical reactivity and solution processability of the 2D superatomic material. After the removal of Cl, $Re_6Se_8(NMF)_{2-x}$ becomes insoluble in NMF and the resulting solid does not dissolve in other common organic solvents (Figure 4A). When the 2D Re_6Se_8 nanosheets are functionalized with SPh, the precipitated solid can be redissolved in DMF (>5 mg/mL) to form a colloid that is stable for at least 2 months at room temperature (Figure 4B). We find that functionalization with $SC_{16}H_{33}$ ligands leads to a more drastic change in colloidal stability and solubility: for instance, we can disperse $Re_6Se_8(SC_{16}H_{33})_2$ in THF (>5 mg/mL) and obtain a colloid that is stable for at least 1 month at room temperature (Figure 4C). This enhanced colloidal stability will broaden the scope of chemical transformations, processing techniques, and thus the applications of these materials that are feasible for these 2D superatomic materials.

By using homolytically cleavable reagents, we controllably surface-functionalized 2D superatomic $Re_6Se_8Cl_2$ monolayers without disrupting their in-plane structure. By activating

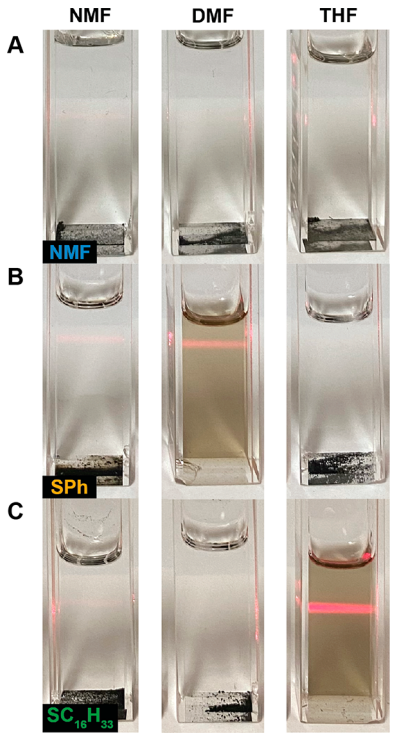

Figure 4. Tyndall scattering of (A) $Re_6Se_8(NMF)_{2-x}$, (B) $Re_6Se_8(SPh)_2$, and (C) $Re_6Se_8(SC_{16}H_{33})_2$ in NMF, DMF, and THF.

$Re_6Se_8Cl_2$ via Li intercalation, we completely removed LiCl from $Li_2Re_6Se_8Cl_2$, yielding 2D $Re_6Se_8(NMF)_{2-x}$. This led us to explore functionalization with homolytically cleavable reagents. Through this strategy, we synthesized four previously unreported 2D superatomic Re_6Se_8 materials that are capped with iodine ($Re_6Se_8I_2$) and thiols ($Re_6Se_8(SR)_2$, where R = Ph, 4-NH_2Ph, $C_{16}H_{33}$). Through a combination of vibrational spectroscopy, EDX, ICP, and high-resolution imaging, we determined that these transformations occur stoichiometrically and do not disrupt the in-plane crystallinity of 2D Re_6Se_8. Surface modification tunes the solubility of Re_6Se_8 nanosheets, allowing a drastic enhancement to the solubility of Re_6Se_8 in organic solvents. We anticipate that controlled surface functionalization will expand the scope of 2D superatomic nanosheets and provide another avenue to tailor their solution processability, chemical reactivity, and physical properties.

■ ASSOCIATED CONTENT

Supporting Information

The Supporting Information is available free of charge at https://pubs.acs.org/doi/10.1021/jacs.1c10833.

Additional experimental details and data as described in the text (PDF)

■ AUTHOR INFORMATION

Corresponding Authors

Xavier Roy − *Department of Chemistry, Columbia University, New York, New York 10027, United States;* orcid.org/0000-0002-8850-0725; Email: xr2214@columbia.edu

Colin Nuckolls − *Department of Chemistry, Columbia University, New York, New York 10027, United States;* orcid.org/0000-0002-0384-5493; Email: cn37@columbia.edu

https://doi.org/10.1021/jacs.1c10833
J. Am. Chem. Soc. 2022, 144, 74−79

Michael L. Steigerwald − *Department of Chemistry, Columbia University, New York, New York 10027, United States*; Email: mls2064@columbia.edu

Authors

Shoushou He − *Department of Chemistry, Columbia University, New York, New York 10027, United States*

Austin M. Evans − *Department of Chemistry, Columbia University, New York, New York 10027, United States*; orcid.org/0000-0002-3597-2454

Elena Meirzadeh − *Department of Chemistry, Columbia University, New York, New York 10027, United States*

Sae Young Han − *Department of Chemistry, Columbia University, New York, New York 10027, United States*

Jake C. Russell − *Department of Chemistry, Columbia University, New York, New York 10027, United States*

Ren A. Wiscons − *Department of Chemistry, Columbia University, New York, New York 10027, United States*

Amymarie K. Bartholomew − *Department of Chemistry, Columbia University, New York, New York 10027, United States*

Douglas A. Reed − *Department of Chemistry, Columbia University, New York, New York 10027, United States*; orcid.org/0000-0001-5170-9050

Amirali Zangiabadi − *Department of Chemistry, Columbia University, New York, New York 10027, United States*

Complete contact information is available at: https://pubs.acs.org/10.1021/jacs.1c10833

Author Contributions

All authors have given approval to the final version of the manuscript.

Notes

The authors declare no competing financial interest.

■ ACKNOWLEDGMENTS

Research into the surface functionalization of 2D materials was supported by the NSF CAREER award DMR-1751949 (X.R.). Work on superatomic materials was supported by the NSF MRSEC on Precision-Assembled Quantum Materials DMR-2011738 and the Air Force Office of Scientific Research award FA9550-18-1-0020 (X.R., C.N., M.L.S.). C.N. thanks Sheldon and Dorothea Buckler for their generous support. A.M.E. is supported by the Schmidt Science Fellows, in partnership with the Rhodes Trust. R.A.W. and A.K.B. were supported by Arnold O. Beckman Fellowships in Chemical Sciences. D.A.R. thanks the Columbia Nano Initiative for postdoctoral fellowship support. The authors acknowledge the Columbia University Shared Materials Characterization Lab (SMCL) and the Electron Microscopy Lab. The authors thank Tai-De Li from the City University of New York for conducting the XPS measurements.

■ REFERENCES

(1) Ryder, C. R.; Wood, J. D.; Wells, S. A.; Yang, Y.; Jariwala, D.; Marks, T. J.; Schatz, G. C.; Hersam, M. C. Covalent functionalization and passivation of exfoliated black phosphorus via aryl diazonium chemistry. *Nat. Chem.* **2016**, *8*, 597−602.

(2) Georgakilas, V.; Otyepka, M.; Bourlinos, A. B.; Chandra, V.; Kim, N.; Kemp, K. C.; Hobza, P.; Zboril, R.; Kim, K. S. Functionalization of Graphene: Covalent and Non-Covalent Approaches, Derivatives and Applications. *Chem. Rev.* **2012**, *112*, 6156−6214.

(3) Tofan, D.; Sakazaki, Y.; Walz Mitra, K. L.; Peng, R.; Lee, S.; Li, M.; Velian, A. Surface Modification of Black Phosphorus with Group 13 Lewis Acids for Ambient Protection and Electronic Tuning. *Angew. Chem., Int. Ed.* **2021**, *60*, 8329−8336.

(4) Boles, M. A.; Ling, D.; Hyeon, T.; Talapin, D. V. The surface science of nanocrystals. *Nat. Mater.* **2016**, *15*, 141−153.

(5) Voiry, D.; Goswami, A.; Kappera, R.; de Carvalho Castro e Silva, C.; Kaplan, D.; Fujita, T.; Chen, M.; Asefa, T.; Chhowalla, M. Covalent functionalization of monolayered transition metal dichalcogenides by phase engineering. *Nat. Chem.* **2015**, *7*, 45−49.

(6) Nguyen, E. P.; Carey, B. J.; Ou, J. Z.; van Embden, J.; Gaspera, E. D.; Chrimes, A. F.; Spencer, M. J. S.; Zhujykov, S.; Kalantar-zadeh, K.; Daeneke, T. Electronic Tuning of 2D MoS_2 through Surface Functionalization. *Adv. Mater.* **2015**, *27*, 6225−6229.

(7) Paredes, J. I.; Munuera, J. M.; Villar-Rodil, S.; Guardia, L.; Ayán-Varela, M.; Pagán, A.; Aznar-Cervantes, S. D.; Cenis, J. L.; Martínez-Alonso, A.; Tascón, J. M. D. Impact of Covalent Functionalization on the Aqueous Processability, Catalytic Activity, and Biocompatibility of Chemically Exfoliated MoS_2 Nanosheets. *ACS Appl. Mater. Interfaces* **2016**, *8*, 27974−27986.

(8) Knirsch, K. C.; Berner, N. C.; Nerl, H. C.; Cucinotta, C. S.; Gholamvand, Z.; McEvoy, N.; Wang, Z.; Abramovic, I.; Vecera, P.; Halik, M.; Sanvito, S.; Duesberg, G. S.; Nicolosi, V.; Hauke, F.; Hirsch, A.; Coleman, J. N.; Backes, C. Basal-Plane Functionalization of Chemically Exfoliated Molybdenum Disulfide by Diazonium Salts. *ACS Nano* **2015**, *9*, 6018−6030.

(9) Chou, S. S.; De, M.; Kim, J.; Byun, S.; Dykstra, C.; Yu, J.; Huang, J.; Dravid, V. P. Ligand Conjugation of Chemically Exfoliated MoS_2. *J. Am. Chem. Soc.* **2013**, *135*, 4584−4587.

(10) Zhong, X.; Lee, K.; Choi, B.; Meggiolaro, D.; Liu, F.; Nuckolls, C.; Pasupathy, A.; De Angelis, F.; Batail, P.; Roy, X.; Zhu, X. Superatomic Two-Dimensional Semiconductor. *Nano Lett.* **2018**, *18*, 1483−1488.

(11) Zhong, X.; Lee, K.; Meggiolaro, D.; Dismukes, A. H.; Choi, B.; Wang, F.; Nuckolls, C.; Paley, D. W.; Batail, P.; De Angelis, F.; Roy, X.; Zhu, X.-Y. $Mo_6S_3Br_6$: An Anisotropic 2D Superatomic Semiconductor. *Adv. Funct. Mater.* **2019**, *29*, 1902951.

(12) Kephart, J. A.; Romero, C. G.; Tseng, C.; Anderton, K. J.; Yankowitz, M.; Kaminsky, W.; Velian, A. Hierarchical nanosheets built from superatomic clusters: properties, exfoliation and single-crystal-to-single-crystal intercalation. *Chem. Sci.* **2020**, *11*, 10744−10751.

(13) Champsaur, A. M.; Yu, J.; Roy, X.; Paley, D. W.; Steigerwald, M. L.; Nuckolls, C.; Bejger, C. M. Two-Dimensional Nanosheets from Redox-Active Superatoms. *ACS Cent. Sci.* **2017**, *3*, 1050−1055.

(14) Telford, E. J.; Russell, J. C.; Swann, J. R.; Fowler, B.; Wang, X.; Lee, K.; Zangiabadi, A.; Watanabe, K.; Taniguchi, T.; Nuckolls, C.; Batail, P.; Zhu, X.; Malen, J. A.; Dean, C. R.; Roy, X. Doping-Induced Superconductivity in the van der Waals Superatomic Crystal $Re_6Se_8Cl_2$. *Nano Lett.* **2020**, *20*, 1718−1724.

(15) Willer, M. W.; Long, J. R.; McLauchlan, C. C.; Holm, R. H. Ligand Substitution Reactions of $[Re_6S_8Br_6]^{4+}$: A Basis Set of Re_6S_8 Clusters for Building Multicluster Assemblies. *Inorg. Chem.* **1998**, *37*, 328−333.

(16) Zheng, Z.; Long, J. R.; Holm, R. H. A Basis Set of Re_6Se_8 Cluster Building Blocks and Demonstration of Their Linking Capability: Directed Synthesis of an $Re_{12}Se_{16}$ Dicluster. *J. Am. Chem. Soc.* **1997**, *119*, 2163−2171.

(17) Doud, E. A.; Voevodin, A.; Hochuli, T. J.; Champsaur, A. M.; Nuckolls, C.; Roy, X. Superatoms in materials science. *Nat. Rev. Mater.* **2020**, *5*, 371−387.

(18) Choi, B.; Lee, K.; Voevodin, A.; Wang, J.; Steigerwald, M. L.; Batail, P.; Zhu, X.; Roy, X. Two-Dimensional Hierarchical Semiconductor with Addressable Surfaces. *J. Am. Chem. Soc.* **2018**, *140*, 9369−9373.

(19) Leduc, L.; Perrin, A.; Sergent, M. Structure du dichlorure et octaséléniure d'hexarhénium, $Re_6Se_8Cl_2$: composé bidimensionnel à clusters octaédriques Re6. *Acta Crystallogr. Sect. C* **1983**, *39*, 1503−1506.

(20) Bruck, A. M.; Yin, J.; Tong, X.; Takeuchi, E. S.; Takeuchi, K. J.; Szczepura, L. F.; Marschilok, A. C. Reversible Electrochemical Lithium-Ion Insertion into the Rhenium Cluster Chalcogenide−Halide $Re_6Se_8Cl_2$. *Inorg. Chem.* **2018**, *57*, 4812−4815.
(21) The detection limits of Li ICP-OES and Cl EDX are 0.01% and 1%, respectively. Therefore, %Li ≤ 0.01% and %Cl ≤ 1%.
(22) Leader, G. R.; Gormley, J. F. The Dielectric Constant of *N*-Methylamides. *J. Am. Chem. Soc.* **1951**, *73*, 5731−5733.
(23) Suzuki, I. Infrared Spectra and Normal Vibrations of *N*-Methylformamides $HCONHCH_3$, $HCONDCH_3$, $DCONHCH_3$ and $DCONDCH_3$. *Bull. Chem. Soc. Jpn.* **1962**, *35*, 540−551.
(24) Mackay, R. A.; Poziomek, E. J. Preparation and Properties of Metal(II) Complexes of *N*-Methylformamide. *Inorg. Chem.* **1968**, *7*, 1454−1457.
(25) Dines, M. B. Lithium intercalation via *n*-Butyllithium of the layered transition metal dichalcogenides. *Mater. Res. Bull.* **1975**, *10*, 287−291.
(26) Brec, R.; Schleich, D. M.; Ouvrard, G.; Louisy, A.; Rouxel, J. Physical Properties of Lithium Intercalation Compounds of the Layered Transition Chalcogenophosphates. *Inorg. Chem.* **1979**, *18*, 1814−1818.
(27) Laing, C. C.; Shen, J.; Chica, D. G.; Cuthriell, S. A.; Schaller, R. D.; Wolverton, C.; Kanatzidis, M. G. Photoluminescent $Re_6Q_8I_2$ (Q = S, Se) Semiconducting Cluster Compounds. *Chem. Mater.* **2021**, *33*, 5780−5789.
(28) The experimental [Re]:[I] is 2.5, which correlates well with the expected [Re]:[I] = 3. This indicates that the Cl to I substitution is nearly stoichiometric.
(29) The experimental [Re]:[S] ratios are 2.6, 2.6, and 2.3 for $Re_6Se_8(SPh)_2$, $Re_6Se_8(SPhNH_2)_2$, and $Re_6Se_8(SC_{16}H_{33})_2$, respectively. The experimental ratios correlate well with the expected [Re]:[S] = 3. This indicates that the Cl to SR substitution is nearly stoichiometric.

https://doi.org/10.1021/jacs.1c10833
J. Am. Chem. Soc. 2022, 144, 74−79